Available online at www.sciencedirect.com
SCIENCE DIRECT®
ELSEVIER
Journal of Crystal Growth 278 (2005) 299–304
JOURNAL OF CRYSTAL GROWTH
www.elsevier.com/locate/jcrysgro

Characterization of ZnO/$Mg_{0.12}Zn_{0.88}O$ heterostructure grown by plasma-assisted molecular beam epitaxy

Y.M. Lu*, C.X. Wu, Z.P. Wei, Z.Z. Zhang, D.X. Zhao, J.Y. Zhang, Y.C. Liu, D.Z. Shen, X.W. Fan

Laboratory of Excited State Processes, Changchun Institute of Optics, Fine Mechanics and Physics, Chinese Academy of Sciences, Changchun 130033, China

Abstract

In this paper, $Mg_{0.12}Zn_{0.88}O$/ZnO heterostructures were fabricated on *c*-plane sapphire (Al_2O_3) substrates by plasma-assisted molecular beam epitaxy (P-MBE). The quality of the $Mg_{0.12}Zn_{0.88}O$ alloy thin film was characterized by X-ray diffraction (XRD) and reflection high-energy electron diffraction (RHEED). Optical properties of the $Mg_{0.12}Zn_{0.88}O$/ZnO heterostructure were studied by absorption and photoluminescence (PL) spectra. At room temperature (RT), $Mg_{0.12}Zn_{0.88}O$/ZnO heterostructures show two absorption edges originating from ZnO and $Mg_{0.12}Zn_{0.88}O$ layers, respectively. In PL spectra, two ultraviolet emission bands related to the ZnO layer and the $Mg_{0.12}Zn_{0.88}O$ layer were observed. The emission band from $Mg_{0.12}Zn_{0.88}O$ layer dominates at moderately lower temperature, and the luminescence of ZnO becomes gradually important with increasing temperature. This is suggested to exist as a potential barrier in the interface and to restrict the relaxation of the carriers from the $Mg_{0.12}Zn_{0.88}O$ layer to ZnO layer. As the thickness of ZnO layer decreases, the emission from the $Mg_{0.12}Zn_{0.88}O$ layer becomes weaker and weaker. When the ZnO thickness is up to 2 nm, only the luminescence of the ZnO layer is observed at RT. The quenching of the emission corresponding to the MgZnO layer indicates the existence of a strong injection process in the samples with thinner ZnO layer.

Keywords: A1. Interface potential barrier; A1. Photoluminescence; A3. Molecular beam epitaxy; B1. ZnO/MgZno; B2. Semiconducting II–VI materials; B3. Heterojunction semiconductor device

1. Introduction

Recently, ZnO-based semiconductors have been attracting increasing attention as promising candidates for optoelectronic applications in ultraviolet

---

*Corresponding author. No. 16, Dong Nanhu Road, Changchun 130033, PR China. Tel.: +86 431 5682964; fax: +86 431 4627031.
E-mail address: ymlu@mail.jl.cn (Y.M. Lu).

0022-0248/$ - see front matter © 2005 Elsevier B.V. All rights reserved.
doi:10.1016/j.jcrysgro.2005.01.023

(UV) regions [1,2]. Because ZnO has a very large exciton binding energy (60 meV), this allows efficient excitonic emission at high temperature [3]. As is well known, an exciton-related lasing process can easily achieve higher gain and lower threshold, ZnO desirable to develop optoelectronic devices based on excitonic effect [4,5]. Additionally, in order to obtain the high-performance light-emitting diodes (LED) devices, one of the key techniques is to construct a heterojunction to realize double confinement actions for electrons and photons in optoelectronic devices. Because the ionic radius of Mg^{2+}(0.57 Å) is close to that of Zn^{2+}(0.6 Å), $Mg_xZn_{1-x}O$ alloy is considered to be a suitable potential barrier material by doping Mg substitute for Zn^{2+} ion in ZnO [6]. Hence, it is necessary to study the growth and characterization of ZnO/$Mg_xZn_{1-x}O$ heterostructure.

Most of the previous works were focused on the fabrication of $Mg_xZn_{1-x}O$ alloy thin films [7–9] and of ZnO/$Mg_xZn_{1-x}O$ heterostructure [10–12] which is essential for band gap engineering as well as device application. In particular, the confirmation of quantum well structure and the luminescence of exciton in low-dimensional structure in which the ultraviolet lasing based on them with low threshold of 11 kW/cm^2 was obtained, were studied in detail [13,14]. However, the effect of heterostructure size on luminescence properties has not been reported yet, although it is important to fabricate the quantum well structure and design the light-emitting device. In this paper, $Mg_{0.12}Zn_{0.88}O$/ZnO heterostructures were grown on (0 0 1) *c*-plane sapphire substrate by P-MBE. The quality of the $Mg_xZn_{1-x}O$/ZnO heterostructure was characterized by measuring XRD, reflection high-energy electron diffraction (RHEED) and optical properties. The optical properties of the heterostructure with different ZnO layer thicknesses were studied, and the luminescence from $Mg_xZn_{1-x}O$ and ZnO layers was observed due to the existence of interface potential barrier. In the heterostructure with thinner ZnO layer, the emission from MgZnO layer was quenched due to strong carrier injection from MgZnO layer to ZnO layer.

2. Experimental procedure

The growth was carried out using a V80H molecular-beam epitaxy (MBE) system equipped with Knudsen-cells for a Zn solid source (99.9999%) and an Mg solid source (99.999%) and radio frequency (rf)-plasma source for oxygen. The background vacuum of the growth chamber was about 1×10^{-10} mbar with a liquid nitrogen supply. The oxygen flow rate is controlled by a leak valve. During growth, the rf power of oxygen plasma was 300 W, the flow rate was kept at 2.0 sccm, and beam fluxes of Zn and Mg were 3.0×10^{-5} and 1.5–3.0×10^{-7} mbar, respectively. The *c*-plane sapphire was used as substrate. In order to obtain a clean fresh surface, the substrates were chemically etched in a hot solution of $H_2SO_4{:}H_3PO_4 = 3{:}1$ at 160 °C for 15 min. Before growth, the substrates were thermally pre-treated at 700 °C for 30 min and exposed to an oxygen plasma at 650 °C for another 30 min, which was expected to remove surface contaminant and obtain oxygen terminated Al_2O_3 (0 0 0 1) surface. The films were grown at 550 °C in the growth pressure of 5.0×10^{-5} mbar. First, a 100 nm thick $Mg_{0.12}Zn_{0.88}O$ buffer layer was grown on sapphire substrate. Then a ZnO layer was sandwiched between the buffer layer and a 30 nm thick $Mg_{0.12}Zn_{0.88}O$ capping layer. Here, the thickness of ZnO layer was varied from 1 to 20 nm.

The samples were characterized by X-ray diffraction (XRD) using a D/max-RA X-ray diffractometer with CuKα_1 line of 1.5418 Å. The transmission spectra were measured by using a xenon lamp with a UV-360 Spectrophotometer. A JY63 Micro Raman spectrometer was employed for PL measurement. The luminescence from the sample was detected by a charged-coupled device (CCD) detector. The excitation source was the 325 nm line of an He–Cd laser with 5 mW power. The liquid-nitrogen cooling system was used in conjunction with the sample stage to cool a sample to 80 K. The temperature was controlled by the TMS94 from 80 K to room temperature (RT).

3. Results and discussion

Fig. 1 shows the XRD spectra of the grown ZnO thin film, $Mg_{0.12}Zn_{0.88}O$ alloy film and $Mg_{0.12}Zn_{0.88}O$/ZnO heterostructure. From Fig. 1a, there are three peaks observed in XRD pattern of the ZnO thin film. The peak at 41.68° is the (0 0 6) diffraction peak of Al_2O_3, and the other two peaks located at 34.44° and 72.72° are attributed to the (0 0 2) and (0 0 4) diffraction peaks of ZnO, respectively. For the $Mg_{0.12}Zn_{0.88}O$ alloy film (Fig. 1b), XRD spectrum shows the same three peaks without another cubic phase, indicating the formation of $Mg_{0.12}Zn_{0.88}O$ alloy film with wurtzite structure. Because Zn^{2+} ions in the ZnO lattice were replaced partly by Mg^{2+} ions with smaller radium, we noted that the (0 0 2) peak of $Mg_{0.12}Zn_{0.88}O$ shifts to 34.57° due to the decrease of the lattice constant along the *c*-plane. Fig. 1c gives the XRD result of $Mg_{0.12}Zn_{0.88}O$/ZnO heterostructure with the thickness of 20 nm ZnO layer. Compared to $Mg_{0.12}Zn_{0.88}O$ alloy film, the (0 0 2)-oriented diffraction peak shows a broadening from 0.16° to 0.21°. This broadening is considered to be due to the superposition of ZnO(0 0 2) and $Mg_{0.12}Zn_{0.88}O$(0 0 2) diffraction peaks, identifying the formation of the ZnMgO/ZnO heterostructure.

Surface and crystal quality of the samples have been investigated by RHEED. Fig. 2 shows RHEED patterns along [1 2 1 0] direction of the substrate exposed to O-plasma at 650 °C for 30 min and the grown ZnO and $Mg_{0.12}Zn_{0.88}O$ thin films. After plasma treatment, the substrate gives a streaky pattern (Fig. 2a), which indicates a well-ordered and flat Al_2O_3 surface. For the grown samples, a change of the RHEED patterns from sharp streaky to discontinuous streaky is observed, as shown in Figs. 2b and c. A sharp streaky pattern shows the formation of smooth and flat surface for the grown ZnO sample, whereas discontinuous streaky pattern indicates that the surface of the $Mg_{0.12}Zn_{0.88}O$ alloy becomes rough. This morphology evolution reveals the effect of lattice disorder due to the introduction of Mg atoms.

Fig. 3 gives RT absorption spectra (a) and PL spectra (b) of the ZnO thin film, $Mg_{0.12}Zn_{0.88}O$ thin film and $Mg_{0.12}Zn_{0.88}O$/ZnO heterostructure with ZnO layer thickness of 20 nm, respectively. For all the samples, the absorption spectra show high transparency in the visible region. ZnO and

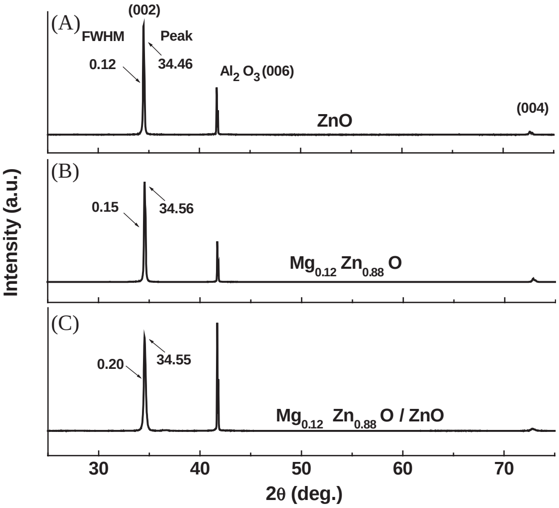

Fig. 1. The X-ray diffraction spectra of the grown ZnO thin film (a), the $Mg_{0.12}Zn_{0.88}O$ alloy thin film (b) and the $Mg_{0.12}Zn_{0.88}O$ /ZnO heterostructure (c).

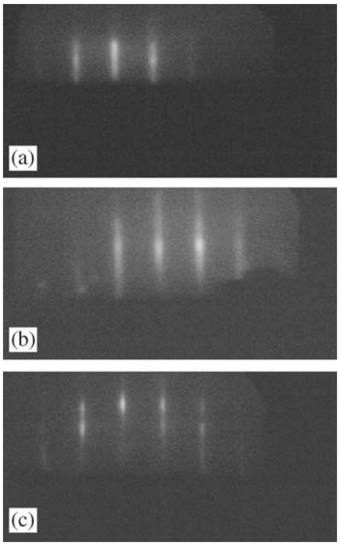

Fig. 2. The RHEED patterns of Al_2O_3 substrate treated by O-plasma (a), the ZnO thin film (b) and the $Mg_{0.12}Zn_{0.88}O$ alloy thin film (c).

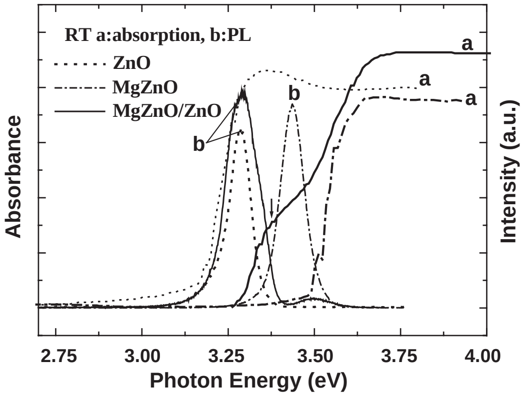

Fig. 3. The absorption spectra (a) and PL spectra (b) of the ZnO and $Mg_{0.08}Zn_{0.92}O$ and $Mg_{0.12}Zn_{0.88}O$ /ZnO heterostructures at RT.

MgZnO thin films have a sharp absorption edge in the ultraviolet (UV) region. For the $Mg_{0.12}Zn_{0.88}O$/ZnO heterostructure, in addition to the absorption edge of MgZnO, a step is observed at about 3.37 eV (arrow in the figure). The appearance of this step indicates the existence of absorption from the ZnO layer in the heterostructure. The RT PL spectra of the above the samples are shown in Fig. 3b. As can be clearly seen, the samples of ZnO and MgZnO show only one emission located at 3.45 and 3.29 eV, respectively. For the $Mg_{0.12}Zn_{0.88}O$/ZnO heterostructure, a stronger emission at 3.29 eV and a weaker emission at 3.50 eV are observed in the spectrum. By comparing the energy positions of the luminescence peaks, these two emission bands in the heterostructure are attributed to the recombinations from the MgZnO layer and the ZnO layer, respectively. It is found that ZnO absorption edge in $Mg_{0.12}Zn_{0.88}O$/ZnO heterostructure exists as an obvious blueshift contrasting with that of ZnO thin film. Because Mg source was heated up all the time during the growth of ZnO layer, although the shutter of Mg source was closed in this process, it was possible that a few Mg atoms emerged from behind the shutter. We suggestion that the ZnO layer in the heterostructure contained a very few Mg atoms, resulting in the blueshift of the ZnO absorption edge in the heterostructure. However, this suggestion cannot explain the coincidence of ZnO PL peak positions from the ZnO thin film and the $Mg_{0.12}Zn_{0.88}O$/ZnO heterostructure. Therefore, it is necessary to understand the origin of these two emissions at RT.

Fig. 4 shows the PL spectra at different temperatures for the ZnO thin film (a) and the $Mg_{0.12}Zn_{0.88}O$/ZnO heterostructure with ZnO layer thickness of 20 nm (b). As the temperature was increased from 80 K to RT, the UV emission of ZnO thin film shifts to low energy side from 3.54 to 3.29 eV.While ZnO luminescence peak of the $Mg_{0.12}Zn_{0.88}O$/ZnO heterostructure shows obvious blueshift with the temperature increase at moderately low temperature (<175 K), the emission peak hardly changes with temperature above 175 K. This means that the above two emissions originate from different luminescence mechanisms. In our earlier work [15], the UV emission of the ZnO thin film was attributed to the

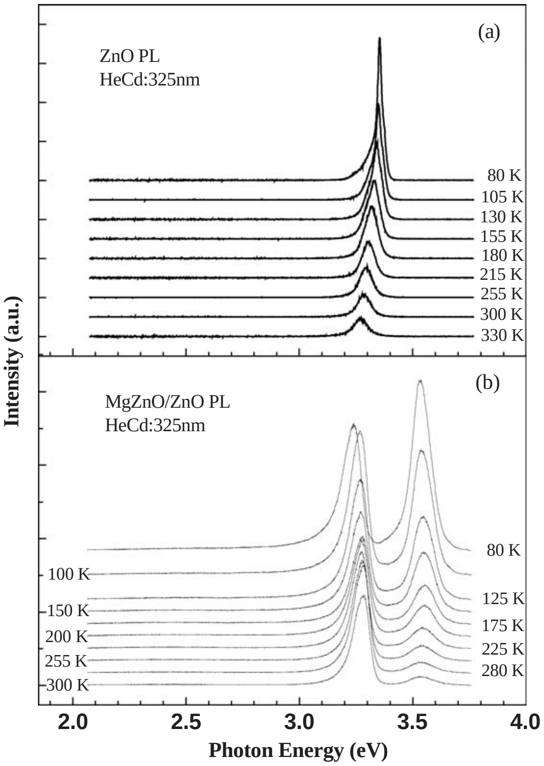

Fig. 4. The PL spectra of the ZnO thin film and the $Mg_{0.12}Zn_{0.88}O$/ZnO heterostructures with ZnO layer thicknesses of 20 nm at different temperatures.

recombination of free excitons with the thermal activation energy of 59 meV, which was in agreement with the exciton binding energy of 60 meV in a bluk ZnO crystal [3]. For the heterostructure, we suggest that the UV emission from ZnO layer originates from the excitons bound to localized states. The excitons bound to localized states in MgZnO/ZnO quantum well had been reported by several groups before [13,14]. These localized states were induced by spatial fluctuations on the relevant heterostructure size. In our samples, because the ZnO layer contained a few Mg atoms, it is possible to form the localized states by the influence of Mg composition fluctuation. From Fig. 4, it is noted that the luminescence from the MgZnO layer in the heterostructure dominates at low temperature (80 K). As the temperature increases to 110 K, the intensity of the MgZnO emission decreases quickly; the intensity of the ZnO emission increases and exceeds that of the MgZnO emission. This implies the existence of a carrier injection process from MgZnO layer to ZnO layer. The ZnO emission in the spectrum becomes gradually important with increasing temperature. This outstanding characteristic of the PL spectrum could be maintained up to room temperature. We considered that there is a potential barrier induced in the interface between MgZnO and ZnO layers. At low temperature (80 K), the interface potential barrier restricts the relaxation of the carriers from MgZnO layer to ZnO layer, resulting in strong MgZnO emission in the spectrum. With increasing temperature, the carriers obtained enough active energy to exceed the barrier and relax into the ZnO layer. The number of the excitons in ZnO layer was increased at moderately low temperature, and the excitons would be bound to the localized states with higher energy due to the carrier injection. Consequently, the ZnO emission is dominant in the spectrum and this emission peak shifts to high energy side with increasing temperature. At higher temperature, this process is redeemed due to the thermal dissociation of the excitons, the emission peak position is not changed with temperature.

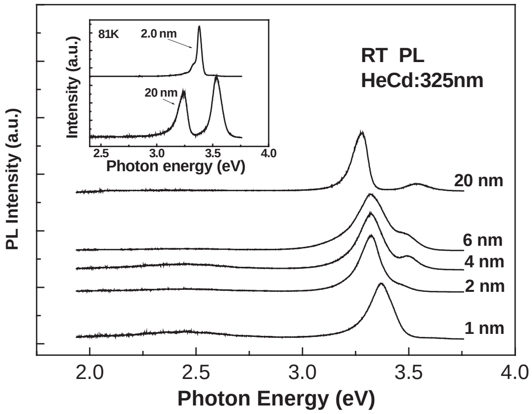

Fig. 5. The PL spectra of the $Mg_{0.12}Zn_{0.88}O/ZnO$ heterostructure with different thicknesses of ZnO layer at RT. The inset shows the PL spectrum of the $Mg_{0.12}Zn_{0.88}O/ZnO$ heterostructures with ZnO layer thicknesses of 2 and 20 nm at 81 K.

In order to further study the formation of the interface potential barrier, we measured RT PL spectra of $Mg_{0.12}Zn_{0.88}O/ZnO$ heterostructures with different ZnO layer thicknesses, as is shown in Fig. 5. When the ZnO layer thickness is 20 nm, it is obvious that the samples show two emission peaks: one is stronger emission from the ZnO layer and another one is weaker emission from the MgZnO layer. As the ZnO layer thickness decreases, the luminescence from the MgZnO layer becomes weaker and weaker, and disappears in ZnO thickness up to 2 nm. For the above samples with thinner ZnO layers, the absorption spectra show only a sharp absorption edge in the ultraviolet region from the MgZnO layer. This means that the emission of the ZnO layer is due to the carrier injection from the MgZnO capping layer to the ZnO layer. This carrier injection process increases with decreasing ZnO layer thickness. Namely, the influence of the interface potential barrier becomes weak with decreasing ZnO layer thickness. The inset of Fig. 5 gives the PL spectrum of $Mg_{0.12}Zn_{0.88}O/ZnO$ heterostructure with ZnO layer thicknesses of 2 and 20 nm at 81 K. It is seen clearly that only one emission peak from the ZnO layer can be observed. In this case, the carriers in the MgZnO layer were completely relaxed to ZnO layer, indicating the disappearance of the interface potential barrier. The possible explanations for the quenching of MgZnO emission could be (1) the tunneling effect resulting in the carrier injection; (2) the strain-induced band gap modification of the ZnO well layer resulting in the disappearance of the interface potential barriers. The detailed reason is not clear at present. The researches on the origin of the interface potential barrier in the heterostructure will be investigated further. From Fig. 5, it is found that UV emission of ZnO shows a clear blueshift with decreasing ZnO layer thickness to 1 nm. Because the exciton Bohr radius of ZnO is ≈18 Å, it means that there exists a strong quantum confinement effect when the ZnO thickness is less than 1.8 nm. For $Mg_{0.12}Zn_{0.88}O/ZnO$ heterostructure with ZnO thickness of 1.0 nm, the quantum well structure with high quality is formed. The nature of mechanism of the ZnO emission in the heterostructure with thinner ZnO layer thickness will be reported elsewhere.

4. Conclusion

In summary, the $Mg_{0.12}Zn_{0.88}O/ZnO$ heterostructure are fabricated on (0 0 1) *c*-plane sapphire substrates by P-MBE. The $Mg_{0.12}Zn_{0.88}O$ alloy thin film with the wurtzite crystal structure is confirmed by XRD and RHEED. Optical properties of $ZnO/Mg_xZn_{1-x}O$ heterostructure is studied by absorption and PL spectra. It is considered that a potential barrier exists in the interface between MgZnO and ZnO layers and confines carrier injection from MgZnO to ZnO layers. With decreasing thickness of the ZnO layer, the increase of carrier injection process results in the disappearance of the luminescence from MgZnO barrier layer.

Acknowledgements

This work is supported by the “863” High Technology Research Program in China, under the Grant No. 2001AA31112, the Innovation Project of Chinese Academy of Sciences, the National Natural Science Foundation of China under Grant Nos. 60336020 and 60278031, and the Program of Hundred Talents of Chinese Academy of Sciences.

References

[1] Y.F. Chen, H.J. Ko, S.K. Hong, T. Yao, Appl. Phys. Lett. 76 (2000) 559.
[2] D.M. Bagnall, Y.F. Chen, Z. Zhu, T. Yao, S. Koyama, M.Y. Shen, T. Goto, Appl. Phys. Lett. 70 (1997) 2230.
[3] D.M. Bagnall, Y.F. Chen, Y.M. Shen, Z. Zhu, T. Goto, T. Yao, J. Crystal Growth 184 (1998) 605.
[4] A. Ohtomo, M. Kawasaki, I. Ohkubo, H. Koinuma, T. Yasuda, Y. Segawa, Appl. Phys. Lett. 75 (1999) 980.
[5] H.D. Sun, T. Makino, N.T. Tuan, Y. Segawa, Z.K. Tang, G.K.L. Wong, H. Koinuma, Appl. Phys. Lett. 77 (2000) 4250.
[6] D.X. Zhao, Y.C. Liu, D.Z. Shen, Y.M. Lu, J.Y. Zhang, X.W. Fan, J. Appl. Phys. 90 (2001) 5561.
[7] S. Choopun, R.D. Vispute, W. Yang, R.P. Sharma, T. Venkatesan, H. Shen, Appl. Phys. Lett. 80 (2002) 1529.
[8] K. Ogata, K. Koike, T. Tanite, T. Komuro, F. Yan, S. Sasa, M. Inoue, M. Yano, J. Crystal Growth (2003) 3327.
[9] S. Muthukumar, J. Zhong, Y. Chen, Y. Lu, T. Siegrist, Appl. Phys. Lett. 82 (2003) 742.
[10] T. Makino, C.H. Chia, N.T. Tuan, H.D. Sun, Y. Segawa, M. Kawasaki, A. Ohtomo, K. Tamura, H. Koinuma, Appl. Phys. Lett. 77 (2000) 975.
[11] S.K. Hong, Y. Chen, H.J. Ko, H. Wenisch, T. Hanada, T. Yao, J. Electron. Mater. 30 (2001) 647.
[12] P. Bhattacharya, R.R. Das, R.S. Katiyar, Appl. Phys. Lett. 83 (2003) 2010.
[13] T. Kakino, C.H. Chia, N.T. Tuan, H.D. Sun, Y. Segawa, M. Kawasaki, A. Ohtomo, K. Tamura, H. Koinuma, Appl. Phys. Lett. 77 (2000) 975.
[14] A. Ohtomo, K. Tamura, M. Kawasaki, T. Makino, Y. Segawa, Z.K. Tang, G.K.L. Wong, Y. Matsumoto, H. Koinuma, Appl. Phys. Lett. 77 (2000) 2204.
[15] W.H. Lang, Y.M. Lu, D.Z. Shen, J.F. Yan, Y.C. Liu, B.H. Li, D.X. Zhao, J.Y. Zhang, X.W. Fan, J. Synth. Cryst. (Chinese) 32 (2003) 579.